Stereoselective Ring-Opening Reaction of Axially Prostereogenic Biaryl Lactones with Chiral Oxazaborolidines: An AM1 Study of the Complete Mechanistic Course†

Gerhard Bringmann* and Daniel Vitt

Institut für Organische Chemie der Universität, Am Hubland, D-97074 Würzburg, Federal Republic of Germany

Received June 20, 1995®

The complete mechanistic course of the atropisomer-selective ring-opening reaction of the axially prostereogenic 1,3-dimethylbenzo[*b*]naphtho[1,2-*d*]pyran-6-one with a chiral oxazaborolidine–BH_3 complex was calculated using the semiempirical AM1 method. It was shown that the high enantioselectivity of the overall reaction is not based on the stereocontrol of the initial attack of the chiral nucleophile but is a consequence of a kinetic atropisomer resolution of the intermediate biaryl aldehydes. The calculated enantioselectivity matches very well with the experimental results, thus demonstrating the suitability of the AM1 method even for these complex mechanistic studies. The results may lead to new, more effective strategies for the enantioselective synthesis of axially chiral biaryl compounds.

Introduction

Axially chiral and configuratively stable biaryl compounds have become increasingly important as effective chiral auxiliaries in stereoselective synthesis[2] and as pharmacologically potent natural products, a prominent example being michellamine B, which exhibits high anti-HIV activity.[3] For this reason, the synthetic availability of nonnatural and natural biaryls in a stereochemically homogeneous form is an important goal.[4] We have developed an efficient concept for the stereoselective synthesis of axially chiral biaryl compounds, in which the aryl coupling step is separated from the introduction of the stereochemical information at the axis,[4–6] thus allowing efficient optimization of both steps independently. First, the two aromatic "halves" **1** and **2** are connected by an ester bridge as in **3** (step A, Scheme 1), allowing an *intramolecular* Pd-catalyzed aryl coupling (step B). Compared with the final target molecules **5**, the resulting biaryl lactones **4** have a dramatically lowered atropisomerization barrier at the axis and hence are stereochemically unstable in most cases.[5,6] Subsequent ring opening of the auxiliary bridge using chiral *N*-, *O*-, *C*-, *S*-, or *H*-nucleophiles[5–8] (step C) atropisomer selectively

Scheme 1

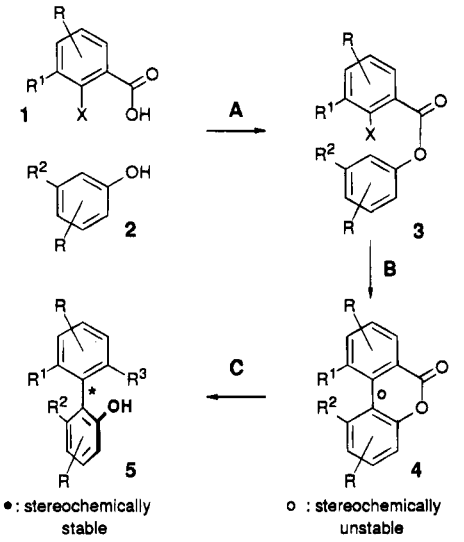

leads to configuratively stable biaryl products **5** with in some cases very high asymmetric inductions.

In previous investigations, benzonaphthopyranones like **6**[9] have proved to be valuable concrete substrates representing the general lactones **4**. For the atropoenantioselective reduction of **6**,[6–8] chiral oxazaborolidines[10] in the presence of BH_3 are highly selective reagents for the realization of our concept. As an example, the reaction of **6** with BH_3 in the presence of the bicyclic oxazaborolidine **7** resulted in the enantioselective formation of the diol (*M*)-**8**,[11] giving an ee of 97%[6–8] (Scheme 2).

On the basis of extensive experimental and kinetic investigations, we have developed a mechanistic hypothesis for the stereochemical course of the ring-opening

* Corresponding author.

† Part 55 of the series "Novel Concepts in Directed Biaryl Synthesis", for part 54 see ref 1.

® Abstract published in *Advance ACS Abstracts,* October 15, 1995.

(1) Lange, J.; Burzlaff, H.; Bringmann, G.; Schupp, O. *Tetrahedron* **1995**, *51*, 9361.

(2) (a) Noyori, R.; Tomino, R.; Tomino, I.; Tanimoto, Y. *J. Am. Chem. Soc.* **1979**, *101*, 3129. (b) Noyori, R.; Tomino, I.; Tanimoto, Y.; Nishizawa, M. *J. Am. Chem. Soc.* **1984**, *106*, 6709. (c) Noyori, R.; Tomino, I.; Yamada, M.; Nishizawa, M. *J. Am. Chem. Soc.* **1984**, *106*, 6717.

(3) (a) McKee, T. C.; Cardellina, J. H., II; Riccio, R.; D'Auria, M. V.; Lorizzi, M.; Minale, L.; Morana, R. A.; Gulakowsi, R. J.; McMahon, J. B.; Buckheit, R. W., Jr.; Snader, K. M.; Boyd, M. R. *J. Med. Chem.* **1991**, *34*, 3402. (b) Boyd, M. R.; Hallock, Y. F.; Cardellina, J. H., II; Manfredi, K. P.; Blunt, J. W.; Mc Mahon, J. B.; Buckheit, R. W., Jr.; Bringmann, G.; Schäffer, M.; Cragg, G. M.; Thomas, D. W.; Jato, J. G. *J. Med. Chem.* **1994**, *37*, 1740.

(4) Bringmann, G.; Walter, R.; Weirich, R. *Angew. Chem.* **1990**, *102*, 1006; *Angew. Chem., Int. Ed. Engl.* **1990**, *29*, 977.

(5) Bringmann, G.; Schupp, O. *S. Afr. J. Chem.* **1994**, *47*, 83.

(6) Bringmann, G.; Göbel, L.; Schupp, O. *GIT Fachz. Lab.* **1993**, *100*, 7891.

(7) Bringmann, G.; Hartung, T. *Angew. Chem.* **1992**, *104*, 782; *Angew. Chem., Int. Ed. Engl.* **1992**, *31*, 761.

(8) Bringmann, G.; Hartung, T. *Tetrahedron* **1993**, *49*, 7891.

(9) Bringmann, G.; Hartung, T.; Göbel, L.; Schupp, O.; Ewers, C. L. J.; Schöner, B.; Zagst, R.; Peters, K.; Peters, E.-M.; von Schnering, H. G.; Burschka, C. *Liebigs Ann. Chem.* **1992**, 225.

(10) (a) Itsuno, S.; Ito, K. *J. Org. Chem.* **1984**, *49*, 555. (b) Corey, E. J.; Bakshi, R. K.; Shibata, S. *J. Am. Chem. Soc.* **1987**, *109*, 5551. (c) Corey, E. J.; Azimioara, M.; Sarshar, S. *Tetrahedron Lett.* **1992**, *33*, 3429. (d) Wallbaum, S.; Martens, J. *Tetrahedron: Asymmetry* **1992**, *4*, 1475.

0022-3263/95/1960-7674$09.00/0

Scheme 2

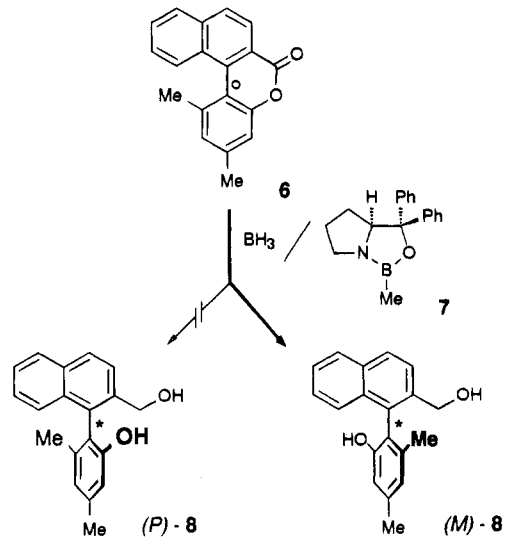

reaction, as shown, in a simplified (merely anionic, metal-free) form in Figure 1.[5,6] Particularly, the complete reduction of **6** (represented by **I**) with chiral oxazaborolidines to the diol **8** (generalized as **IV**) requires two stepwise nucleophilic attacks by the hydride species. The four diastereomeric lactolates **II** that could possibly be formed by a nucleophilic attack and subsequent cleavage of the endocyclic C–O bond can lead to the two enantiomeric aldehydes (*M*)- and (*P*)-**III**. A second hydride-transfer reaction would then deliver the two possible enantiomeric end products **IV**.

According to our hypothesis, the observed excellent asymmetric inductions might result from a highly selective initial attack of the hydride-transfer reagent to the lactone carbonyl group such that only one of the four possible stereoisomeric lactolates **II** could be formed, *e.g.* only (*R,M*)-**II**. This intermediate would then burst open to give (*M*)-**III**, whose further reduction would give rise to (*M*)-**IV**—provided that no loss of stereochemical information,[4] the so-called stereochemical leakage,[8,12] would play a crucial role, *e.g.* by helimerization of (*R,M*)-**II** to (*R,P*)-**II**, thus finally giving rise also to (*P*)-**III** and thus (*P*)-**IV**. A further loss of stereochemical information might arise from the enhanced reactivity of the aldehyde function of (*M*)-**III** compared with the amine functionality previously investigated,[5] so that the already ring-opened species (*M*)-**III** might cyclize again, not only to (*R,M*)-**II**, but also to (*S,M*)-**II**. The more or less rapid helimerization of these cyclic and thus configuratively unstable intermediates might then likewise lead to (*P*)-**III** and thus (*P*)-**IV**.

For the selectivity of the initial formation of only one lactolate, *e.g.* (*R,M*)-**II**, different principles of stereocontrol are imaginable, such as the attack of the hydride-transfer reagent to only one of the two lactone enantiomers [here only to (*M*)-**I**]; second, the attack of the reagent *e.g.* from an axial, rather than from an equatorial direction; and third (and simultaneously the result of the first two principles), the diastereofacial-differentiating reaction *e.g.* only from the *Re* side of the carbonyl function. The rapid isomerization (*M*)-**I** ⇌ (*P*)-**I** would allow a constant supply with (*M*)-**I**, by equilibration of the remaining, since less reactive, (*P*)-**I** enantiomer.

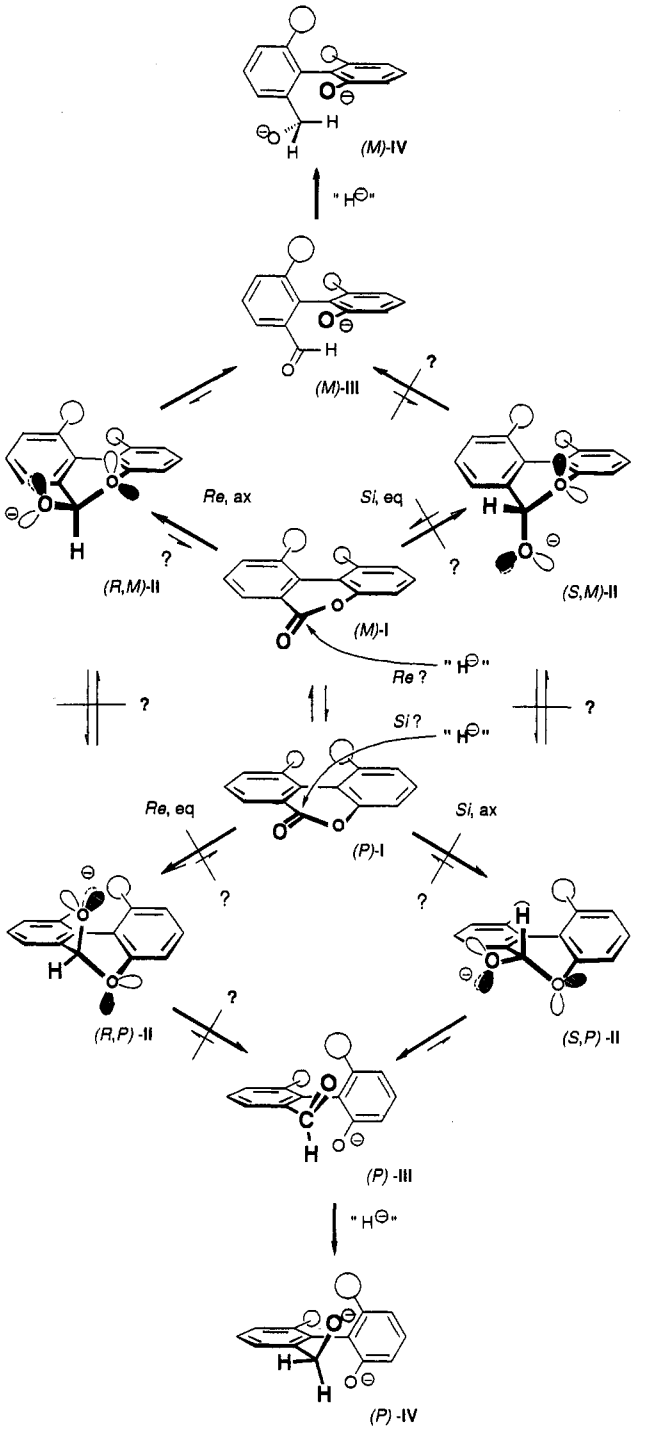

Figure 1. Mechanistic working hypothesis for the atropisomer-selective ring cleavage of configuratively unstable biaryl lactones **1** to give configuratively stable alcohols **IV**. For the CIP denotion, the generalized substituents (marked as O) have arbitrarily been attributed lower priority compared with the concrete ones.

For a further improvement of the obtained preparative results, a better mechanistic understanding of this unprecedented atropisomer-selective cleavage of configuratively unstable biaryl lactones to chiral biaryl target

(11) For the now strongly recommended *M/P* denotion for axial chirality see: (a) Prelog, V.; Helmchen, G. *Angew. Chem.* **1982**, *94*, 614. Prelog, V.; Helmchen, G. *Angew. Chem., Int. Ed.* **1982**, *21*, 567. (b) Helmchen, G. In *Methods of Organic Chemistry (Houben-Weyl)*; Helmchen, G., Hoffmann, R. W., Mulzer, J., Schaumann, E., Eds.; Thieme: Stuttgart, New York, 1995; p 1.

(12) Bringmann, G.; Ewers, C.; Göbel, L.; Hartung, T.; Schöner, B.; Schupp, O.; Walter, R. In *Stereoselective Reactions of Metal-Activated Molecules*; Werner, H., Griesbeck, A. G., Adam, W., Bringmann, G., Kiefer, W., Eds.; Vieweg: Braunschweig, 1992; p 183.

molecules, would be highly desirable. In this paper, we report on the calculation of the fundamental key steps of the proposed mechanism of this important reaction, including conformational isomerization processes, as well as the relevant bond formation and cleavage processes.

Within the complex proposed mechanistic course of the atropisomer-selective cleavage of configuratively unstable lactones, a key role is occupied by the two reduction steps, whereby the first one, the attack of the hydride-transfer reagent to the prostereogenic lactone functionality of **I** (respectively **6**), has so far been considered as the stereochemically determining step of the overall process,[6,8] which was verified for related reactions with chiral *N*-nucleophiles.[5]

For the enantioselective reduction of ketones by oxazaborolidine–BH_3 adducts, computational investigations by means of semiempirical and *ab initio* methods have been described in the literature. Thus, Nevalainen has intensively calculated the conformations of possible intermediates involved in the oxazaborolidine-catalyzed ketone reduction,[13] using *ab initio* RHF/6-31G and RHF/3-21G calculations. Still, it was never proven whether the species calculated are true mechanistic intermediates that are really involved because no transition structures were calculated. First actual mechanistic calculations were performed by Liotta and Jones[14] using the semiempirical MNDO method. This work, however, focused on the hydride-transfer step, exclusively, with neglect of further mechanistically relevant steps, such as the initial complexation and the dissociation of the reaction product. Their results revealed that the geometries of the energetically lowest transition structures for this attack on several prostereogenic ketones correspond to chair conformations.

Further investigations on the stereoselective oxazaborolidine reduction mechanism were published by Williams *et al.*, who calculated the complete catalytic cycle of the reduction of acetone with a chiral oxazaborolidine–BH_3 model adduct.[15] They demonstrated the amazingly high quality of the semiempirical AM1 method concerning parameters and energies of a chiral oxazaborolidine–BH_3 adduct compared with MP2/6-31G* *ab initio* values.[16]

For the analysis of the mechanism of the atropisomer-selective ring-cleavage reaction with particular emphasis on the stereochemical course of the reaction, the use of too strongly simplified model compounds did not seem appropriate. Therefore the calculations were performed on the reaction of the authentic axially prostereogenic lactone **6** with the concrete chiral oxazaborolidine **9**.[17]

Computational Methods

The semiempirical AM1 calculations were performed on Silicon Graphics IRIS 4D/310 GTX, INDIGO (R4000), and i486-LinuX workstations using the VAMP 5.0 and VAMP 5.5[18] programs. The input geometries for the AM1 calculations were obtained by using the TRIPOS force field within the SYBYL program package.[19] Conformational analyses on all minimum geometries were done using the SYBYL RANDOMSEARCH algorithm. Ground structures were minimized by applying the EF algorithm[20] with a gradient norm specification of 0.01 mdyn/Å, whereas transition structures were optimized by the NS01A algorithm[21] using the corresponding keywords of the VAMP program package. Starting geometries for the optimization of transition structures on more complex potential energy surfaces were determined using ADAPTIVSEARCH, an efficient new scanning algorithm for the rapid and economic evaluation of potential surfaces.[22,23] Force calculations were applied to characterize minima and transition structures by calculation of their normal vibrations.

In all cases, the correspondence of transition structures to their local minima was determined by IRC calculations.

Results and Discussion

In a recent paper, we have presented an extensive study of structures and dynamics of lactones like **6**, the starting materials on the reduction.[24] The course of the stereoselective ring-opening reaction of these lactones as investigated in this paper was roughly subdivided into the following fundamental steps: adduct formation from the substrate **6** and the active hydride species **9**, the intramolecular C,H-bond formation ("the first nucleophilic attack"), the conformational behavior of the lactol derivatives **12** (corresponding to the lactolates **II**), and their reversible ring cleavage to hydroxy aldehydes **14** (corresponding to the generalized species **III**) and, finally, their irreversible further reduction to the diol adducts **15** (as concrete representatives of **IV**). In the following, the calculated reaction mechanism is presented in this order.

Formation of the Lactone–Oxazaborolidine Adduct 11. The first elemental reaction step to be calculated was the formation of the Lewis acid–Lewis base adduct **10** from **6** and **9**. These calculations started from the very weakly bonded van der Waals adduct of the active hydride species **9** and the lactone **6**. Due to the fact that in contrast to the enantiomerically pure compound **9**, the lactone **6** is used as a 1:1 mixture of the rapidly interconverting ($\Delta H^{\ddagger}$ = 18.3 kcal/mol,[24] see Table 2) enantiomeric helimers (*M*)-**6** ⇌ (*P*)-**6**, the reaction of **9** with both lactone enantiomers has to be taken into account. As shown in Table 2, the activation barrier for the Lewis acid–Lewis base adduct formation process **6·9** → **10** was found to be 15.3 kcal/mol for the *M*-helimer and 15.4 kcal/mol for the *P*-isomer, respectively. Unexpectedly, the formation of this adduct **10** is distinctly endothermic relative to the corresponding van der Waals

(13) (a) Nevalainen, V. *Tetrahedron: Asymmetry* **1991**, *2*, 63. (b) Nevalainen, V. *Tetrahedron: Asymmetry* **1992**, *3*, 933. (c) Nevalainen, V. *Tetrahedron: Asymmetry* **1993**, *4*, 1505. (d) Nevalainen, V. *Tetrahedron: Asymmetry* **1994**, *5*, 395.

(14) Liotta, D. C.; Jones, D. K. *J. Org. Chem.* **1993**, *58*, 799.

(15) Linney, L. P.; Self, C. R.; Williams, I. H. *J. Chem. Soc., Chem. Commun.* **1994**, 1651.

(16) Linney, L. P.; Self, C. R.; Williams, I. H. *Tetrahedron: Asymmetry* **1994**, *5*, 813.

(17) The formal charges at the boron, nitrogen, and oxygen atoms are neglected in all schemes for reasons of clarity.

(18) Rauhut, G.; Chandrasekhar, J.; Alex, A.; Beck, B.; Sauer, W.; Clark, T.; VAMP 5.5, available from Oxford Molecular Limited, The Magdalen Centre, Oxford Science Park, Sandford on Thames, Oxford OX4 4GA, England.

(19) SYBYL: Tripos Associates, 1699 St. Hanley Road, Suite 303, St. Louis, MO, 63144.

(20) (a) Baker, J. *J. Comput. Chem.* **1986**, *7*, 385. (b) Baker, J. *J. Comput. Chem.* **1987**, *8*, 563.

(21) Powell, M. J. D. *Nonlinear Optimization*; Academic Press: New York, 1982.

(22) Birken, K.; Helf, C.; Küster, U.; Gulden, K.-P.; Stahl, M.; Bringmann, G. *Benutzerinform. Rechenzentr. Univ. Stuttgart* **1994**, *12*, 4.

(23) Bringmann, G.; Gulden, K.-P.; Vitt, D.; Birken, K.; Helf, C. *J. Mol. Modeling* **1995**, *1*, 142–152.

(24) Bringmann, G.; Busse, H.; Dauer, U.; Güssregen, S.; Stahl, M. *Tetrahedron* **1995**, *51*, 3149.

Table 1. Relative Heats of Formation ΔH_{rel}[a] (kcal/mol) and Number of the Imaginary Frequencies (n_i) of the Lactone/Borane Adducts[b]

species	ΔH_{rel}	$\Delta\Delta H_{rel}$	n_i
6 + **9**[c]	−10.2	−10.2[d]	0
(*M*)-**6·9**	−11.9	0.2[d]	0
(*P*)-**6·9**	−12.1	≡0	0
(*M*)-**10**	≡0	≡0	0
(*P*)-**10**	0.5	0.5[e]	0

[a] ΔH_{rel} values relative to (*M*)-**10**. [b] Only the conformers lowest in energy are presented. [c] The *endo* boron atom of **6** and the carbonyl oxygen atom of **9** are separated by 12 Å. [d] Relative to (*P*)-**6·9**. [e] Relative to (*M*)-**10**.

Table 2. Relative Heats of Formation ΔH_{rel} (kcal/mol), Zero Point Energies (ZPE) (kcal/mol), Imaginary Frequencies ν_i (i·cm^{-1}), and Number of the Imaginary Frequencies (n_i) of the Transition Structures of the Adduct Formation Step and of the Atropisomerization Process of 10

transition structure	ΔH_{rel}	$\Delta\Delta H_{rel}$	n_i	ν_i	ZPE	$\Delta H^{\ddagger}$
TS[(*M*)-**6·9** → (*M*)-**10**]	3.4[a]	0.2[b]	1	117.0	424.6	15.3[c]
TS[(*P*)-**6·9** → (*P*)-**10**]	3.3[a]	≡0	1	71.2	424.5	15.4[d]
TS[(*M*)-**10** → (*P*)-**10**]$_A$	18.1[a]	≡0	1	84.6	425.6	18.1[e]
TS[(*M*)-**10** → (*P*)-**10**]$_B$	18.9[a]	0.8[f]	1	83.3	425.5	18.9[e]
TS[(*P*)-**6** → (*M*)-**6**][g]	16.2	–	1	81.7	–	18.3

[a] ΔH_{rel} values relative to (*M*)-**10**. [b] Relative to TS[(*P*)-**6·9** → (*P*)-**10**]. [c] Relative to (*M*)-**6·9**. [d] Relative to (*P*)-**6·9**. [e] Relative to (*M*)-**10**. [f] Relative to TS[(*M*)-**10** → (*P*)-**10**]$_A$. [g] See ref 24.

adducts, by 11.9 kcal/mol for (*M*)-**10** and 12.6 kcal/mol for *P*-**10** (Table 1).[25] This is probably a consequence of the high rigidity of the two reaction partners, **6** and **9**, so that apparently, the repulsion of the two molecular frameworks overcompensates the exothermicity of the Lewis interaction.

The calculated difference in the heats of formation between the two diastereomeric adducts (*M*)- and (*P*)-**10** is 0.5 kcal/mol (Table 1), showing a significant influence of the chirality of the Lewis acid **9** on energies and structures of the helimeric lactone conformations.

In agreement with former investigations on the influence of *achiral* Lewis acid coordination to the ground structures of these lactones,[26,27] again a distinct shortening of the endocyclic C−O bond and an increase of the exocyclic C−O bond length is observable. Another remarkable structural effect is a planarization of the central pyranon ring, thus leading to a higher conjugation between the two aromatic systems. Still, this does not result in a decreased overall helicity of the molecule, as quantified by the sum of the dihedral angles in the "inner spiral loop",[9] because the effect is compensated by a larger twisting of the rest of the molecule.

As for other Lewis acid adducts of related biaryl lactones,[26,27] the activation barrier ($\Delta H^{\ddagger}$ = 18.1 kcal/mol, see Table 2) for the isomerization process (*M*)-**10** ⇌ (*P*)-**10** is slightly ($\Delta\Delta H^{\ddagger}$ = 0.2 kcal/mol) lower for the complex **10** than for the free lactone **6**. We have recently found two energetically identical, since enantiomeric transition structures for the interconversion (*M*)-**6** ⇌ (*P*)-**6**, which is an enatiomerization process[24] (Scheme 3). Due to the presence of the chiral Lewis acid part, the atropisomeric adducts (*M*)-**10** and (*P*)-**10** are diastereomeric. Consequently, the transition structures for their interconversion TS[(*M*)-**10** ⇌ (*P*)-**10**]$_A$ and TS[(*M*)-**10** ⇌ (*P*)-**10**]$_B$ are diastereomeric, too, and differ by 0.8 kcal/mol (see Table 2).

Scheme 3

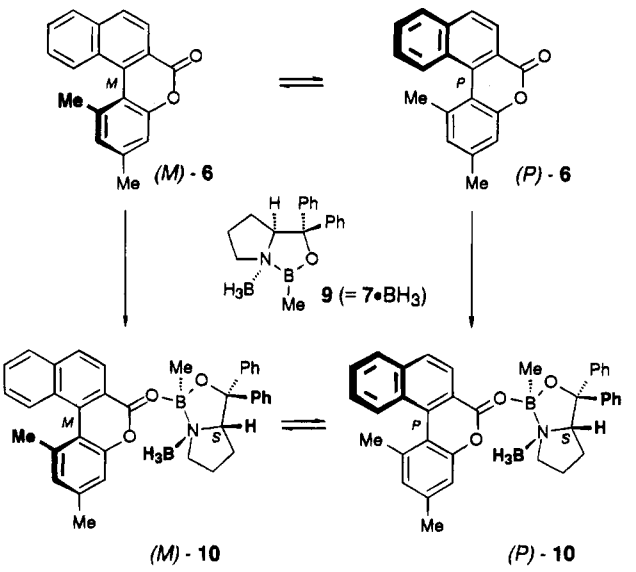

Scheme 4

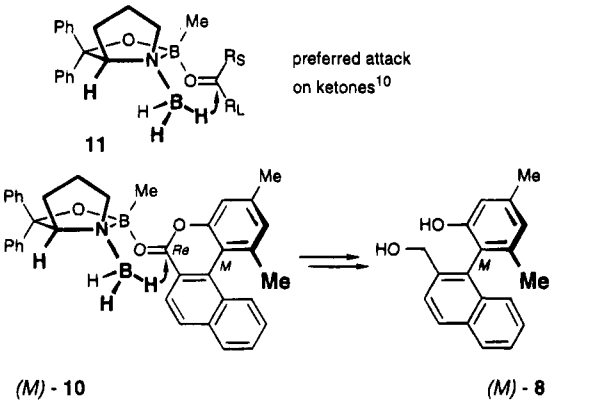

The First Nucleophilic Attack. In contrast to the atropisomer-selective ring-opening reaction investigated in this paper, the stereochemical course of the attack of hydride transfer reagents to *ketone* substrates is more straightforward to analyze experimentally, since the stereochemical information can directly be read from the product, *i.e.* the secondary alcohol, whereas in the reaction sequence discussed here, the intermediately occurring stereocenter is destroyed during the subsequent ring-opening reaction. From that work on structurally related ketones (see the postulated[10c] transition state **11**), the analogous attack on the lactone would have to be expected to occur from the *Re* face, preferentially[28] (Scheme 4).

Furthermore, in analogy to related theoretical work with chiral *N*-nucleophiles,[5] the attack of the hydride-transfer reagent should occur from an axial rather than from an equatorial direction, also for *H*-nucleophiles. Indeed, the calculations show that the distinctly preferred reaction pathway ($\Delta H^{\ddagger}$ = 3.6 kcal/mol, see Table

(25) In the following, all heats of formation are values relative to the Lewis acid/base complex (*M*)-**10**.

(26) Brigmann, G.; Dauer, U.; Schupp, O.; Lankers, M.; Popp, J.; Posset, U.; Weippert, A.; Kiefer, W. *Inorg. Chim. Acta* **1994**, *222*, 247.

(27) Bringmann, G.; Dauer, U.; Lankers, M.; Popp, J.; Posset, U.; Kiefer, W. *J. Mol. Struct.* **1995**, *349*, 431.

(28) Note that, despite the stereochemically analogous array of the two carbonyl substrates, the *Re*/*Si* descriptors will in most cases be opposite for the ketone and the lactone functionalities **11** and (*M*)-**10**, respectively.

Table 3. Relative Heats of Formation ΔH_{rel}[a] (kcal/mol) and Number of the Imaginary Frequencies (n_i) of the Diastereomers for the Minimum Structures Involved in the Reaction Mechanism[b]

species	ΔH_{rel}	$\Delta\Delta H_{rel}$	n_i
(*R*,*M*)-**12**	−37.9	2.9[c]	0
(*S*,*M*)-**12**	−38.5	1.5[c]	0
(*R*,*P*)-**12**	−40.0	≡0	0
(*S*,*P*)-**12**	−37.6	2.4[c]	0
(*R*,*M*)-**13**	−25.4	1.0[d]	0
(*S*,*M*)-**13**	−23.3	3.1[d]	0
(*R*,*P*)-**13**	−26.4	≡0	0
(*S*,*P*)-**13**	−23.8	2.6[d]	0
(*M*)-**14**	−31.1	≡0	0
(*P*)-**14**	−23.6	7.5[e]	0
(*M*)-**15**	−66.8	≡0	0
(*P*)-**15**	−62.9	3.9[f]	0

[a] ΔH_{rel} values relative to (*M*)-**10**. [b] Only the conformers lowest is energy are presented. [c] Relative to (*R*,*P*)-**12**. [d] Relative to (*R*,*P*)-**13**. [e] Relative to (*M*)-**14**. [f] Relative to (*M*)-**15**.

Table 4. Relative Heats of Formation ΔH_{rel}[a] (kcal/mol), Zero Point Eneriges (ZPE) [kcal/mol], Imaginary Frequencies ν_i (i·cm^{-1}), and Number of the Imaginary Frequencies (n_i) of the Transition Structures Involved in the Hydride-Transfer Reactions

transition structure	ΔH_{rel}	$\Delta\Delta H_{rel}$	n_i	ν_i	ZPE	$\Delta H^{\ddagger}$[b]
TS[(*M*)-**10** → (*R*,*M*)-**12**]	3.6	≡0	1	444.3	424.3	3.6
TS[(*M*)-**10** → (*S*,*M*)-**12**]	7.5	3.9[c]	1	457.3	424.1	7.5
TS[(*P*)-**10** → (*R*,*P*)-**12**]	5.7	2.1[c]	1	486.4	424.3	5.2
TS[(*P*)-**10** → (*S*,*P*)-**12**]	5.9	2.3[c]	1	457.3	424.3	5.4
TS[(*R*,*M*)-**12** → (*R*,*M*)-**13**]	−21.5	≡0	1	269.6	426.4	16.4
TS[(*S*,*M*)-**12** → (*S*,*M*)-**13**]	−17.1	4.4[d]	1	253.8	426.6	21.4
TS[(*R*,*P*)-**12** → (*R*,*P*)-**13**]	−20.4	1.1[d]	1	290.4	426.5	19.6
TS[(*S*,*P*)-**12** → (*S*,*P*)-**13**]	−19.7	1.8[d]	1	239.1	426.5	17.9
TS[(*R*,*M*)-**13** → (*M*)-**14**]	−22.5	≡0	1	347.7	425.3	15.4
TS[(*S*,*M*)-**13** → (*M*)-**14**]	−13.5	9.0[e]	1	251.3	425.8	25.0
TS[(*R*,*P*)-**13** → (*P*)-**14**]	−20.0	2.5[e]	1	301.7	425.5	20.0
TS[(*S*,*P*)-**13** → (*P*)-**14**]	−17.6	4.9[e]	1	283.3	425.4	20.0
(*Re*)-**TS**[(*M*)-**14** → (*M*)-**15**]	−11.7	0.3[f]	1	526.6	424.5	28.3[g]
(*Si*)-TS[(*M*)-**14** → (*M*)-**15**]	−12.0	≡0	1	377.5	425.2	28.0[g]
(*Re*)-TS[(*P*)-**14** → (*P*)-**15**]	−3.5	8.5[f]	1	623.1	424.9	36.5[g]
(*Si*)-TS[(*P*)-**14** → (*P*)-**15**]	−8.5	3.5[f]	1	576.4	424.7	31.5[g]

[a] ΔH_{rel} values relative to (*M*)-**10**. [b] $\Delta H^{\ddagger}$ values are related to the corresponding minima. [c] Relative to TS[(*M*)-**10** → (*R*,*M*)-**12**]. [d] Relative to TS[(*R*,*M*)-**12** → (*R*,*M*)-**13**]. [e] Relative to TS[(*R*,*M*)-**13** → (*M*)-**14**]. [f] Relative to (*Si*)-TS[(*M*)-**14** → (*M*)-**15**]. [g] Relative to (*R*,*P*)-**12**.

4) is the axial *Re* attack on the *M* atropisomer of **10**, which can be clearly seen from the corresponding transition structure TS [(*M*)-**10** → (*R*,*M*)-**12**] as shown in Figure 2.

Both, the *Re*- and the axial-type selectivities, are important factors, since the energetically next transition structures ($\Delta H^{\ddagger}$ = 5.2 and 5.4 kcal/mol, see Table 4) correspond to the equatorial but still *Re*-type oriented TS [(*P*)-**10** → (*R*,*P*)-**12**] and the axial but *Si*-type TS [(*P*)-**10** → (*S*,*P*)-**12**] showing that among these principles, the hydride transfer is slightly preferentially controlled by the *Re* topicity of the lactone substrate rather than by the principle of an axial attack. By contrast, the fourth possible reaction pathway, via TS [(*M*)-**10** → (*S*,*M*)-**12**] ($\Delta H^{\ddagger}$ = 7.5 kcal/mol) apparently plays no significant role (see Table 4).

The transition structures resulting from the *Re* attack all have chair conformations, whereas those resulting from a *Si* attack adopt twist boat conformations (Figure 2). Possibly for that reason, the *Si* attack transition structures are significantly higher (2.3 kcal/mol for TS [(*P*)-**10** → (*S*,*P*)-**12**] and 3.9 kcal/mol for TS [(*M*)-**10** → (*S*,*M*)-**12**] in energy (Table 4) than the corresponding *Re* attacks via chair conformations (Scheme 5).

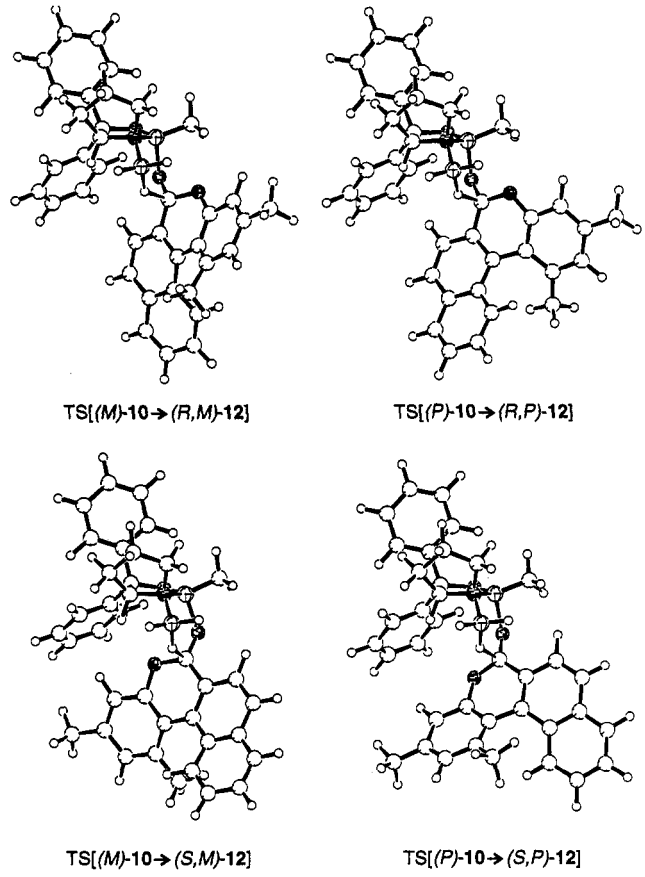

Figure 2. Transition structures for the first hydride-transfer step TS[**10** → **12**] as calculated with AM1. For reasons of clarity, the structures were plotted in a different orientation compared with the formula schemes.

Scheme 5

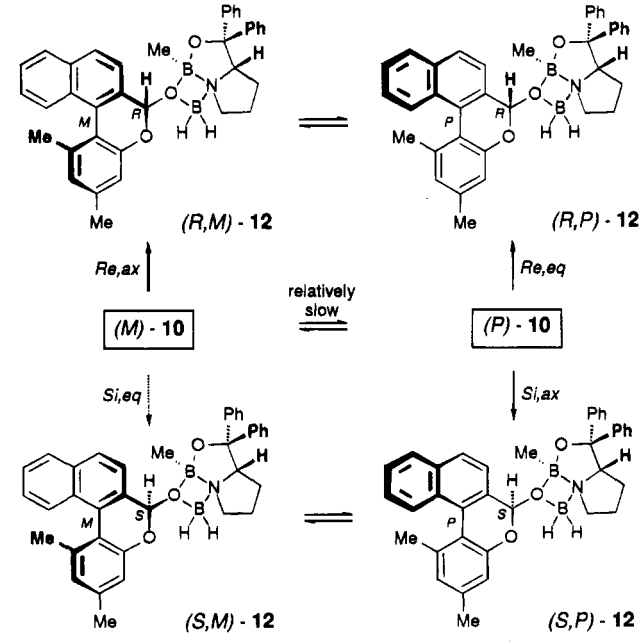

The Lactolate Intermediates 12 and 13—Isomerization and Ring-Cleavage Processes. Despite the expected stereoselectivities that should arise from the different activation barriers for the above-calculated first hydride-transfer reaction to the lactone functionality, these barriers are low compared with the atropisomerization barriers of the precursor **10**, which is thus

configuratively stable within the time scale of the reduction step. This clearly should allow both atropisomers of **10** to be reduced independently, thus giving rise not only to one particular product, but to (*R,M*)-**12**, (*R,P*)-**12**, and (*S,P*)-**12**, predominantly.

An essential characteristic of the oxazaborolidines are its possible coordination positions. Interestingly, the energetically most favored products of the first hydride attack show a coordination of the BH_3-derived boron to the exocyclic oxygen as in **12**, thus giving rise to a four-membered diboraheterocycle. These oxazadiboretane-type products[13] are distinctly more stable (Table 3) than the six-membered isomers **13**, in which the boron is coordinated to the endocyclic oxygen of the previous lactone bridge. Still, the formation of these energetically disfavored heterocyclic isomers **13** is an important precondition for the subsequent ring-opening process (see below); therefore, their formation from **12** was likewise thoroughly investigated. Using the scanning algorithm ADAPTIVSEARCH[22,23] for the location of the starting geometries, we exclusively found transition structures representing a two-step mechanism of **12** → **14** via **13**. For all of the four diastereomeric forms of **12**, the respective transition structures of this coordinative change of the boron atom from the exo- to the endocyclic oxygen atom were located.

The relevance of the energetically less favored six-membered heterocyclic intermediate **13** for the ring-opening process was shown by the fact that, for the (computational) conversion of **12** into **14**, in each case a two-step mechanism was found, consisting of a change of coordination via the transition structure TS[**12** → **13**], followed by the actual ring opening reaction via TS[**13** → **14**] (Table 4). No evidence for a direct, *i.e.* synchronical, process was obtained.

Within this ring-opening reaction **13** → **14** (Scheme 6), we found that the energetically lowest reaction path is a process with a lengthening (and final rupture) of the endocyclic C–O bond, accompanied by a shortening of the bond between the *exo* boron atom and the phenolate oxygen from 179 pm [for (*R,M*)-**13**] to 147 pm [for (*M*)-**14**]. The relative energies for the corresponding transition structures are presented in Table 4.

Besides the constitutional aspects of these chemical reactions, their stereochemical course plays an important role, too. Like the free lactone substrate **6**,[24] the atropisomeric intermediate lactolates **12** (and **13**) can isomerize at the axis within the time scale of the overall reaction if the barrier for one of the following reaction steps is distinctly higher in energy. The activation energies for these atropisomerization processes are within a range of 16.8 for TS [(*R,P*)-**12** → (*R,M*)-**12**] to 20.9 kcal/mol for TS-[(*S,M*)-**13** → (*S,P*)-**13**] (see Table 5) and thus comparable to that of the free lactone **6** (18.3 kcal/mol).[24] In contrast to the atropisomerization process of the latter, which proceeds via two enantiomeric transition structures,[24] two diastereomeric transition structures were found for the helimerization of **12**. As a consequence of the additional stereogenic center, these structures distinctly differ in energy (*e.g.* $\Delta\Delta H$ = 4.5 kcal/mol for TS[(*R,M*)-**12** → (*R,P*)-**12**]$_A$ and TS[(*R,M*)-**12** → (*R,P*)-**12**]$_B$, see Table 5) so that only the lower one ($\Delta H^{\ddagger}$ = 16.8 kcal/mol) has to be taken into account.

Given the likewise easy cyclization of *e.g.* (*P*)-**14** to either (*S,P*)-**13** ($\Delta H^{\ddagger}$ = 6.0 kcal/mol) or (*R,P*)-**13** ($\Delta H^{\ddagger}$ = 3.6 kcal/mol) (see Tables 3 and 4) and the relatively high activation barrier for the second hydride transfer step (see below), both the stereogenic axis and the benzylic stereocenter of **12** have to be considered as unstable within the time scale of the reaction. Hence, the long postulated "stereochemical leakage"[8,12] plays an even more imporatant role than anticipated.

Scheme 6

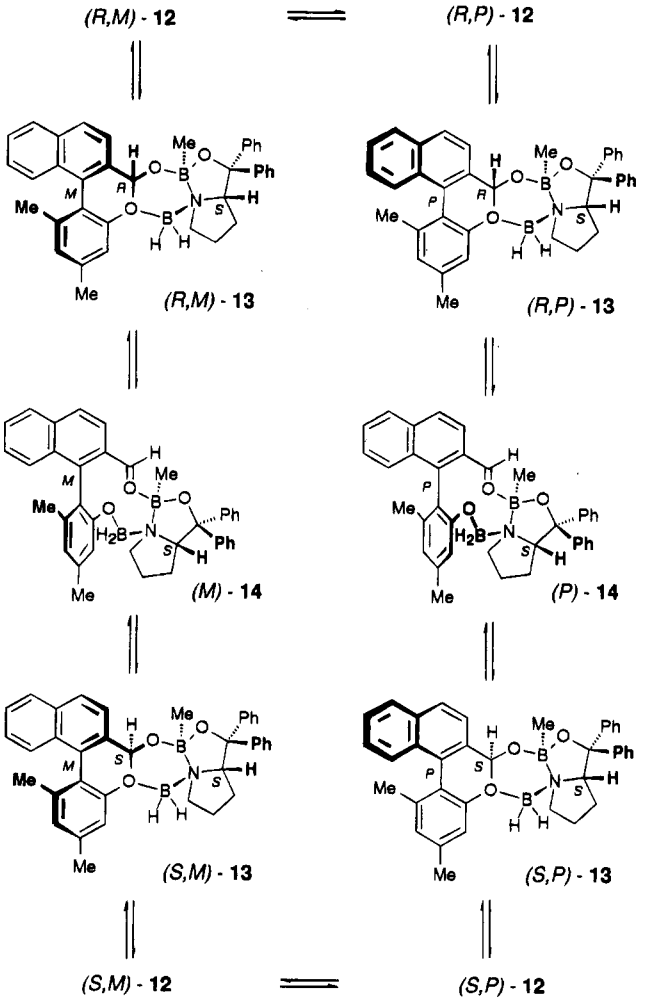

Table 5. Relative Heats of Formation ΔH_{rel}[a] (kcal/mol), Zero Point Eneriges (ZPE) (kcal/mol), Imaginary Frequencies ν_i (i·cm^{-1}), and Number of Imaginary Frequencies (n_i) of the Transition Structures for the Atropisomerization of the Different Lactolate Isomers 12 and 13

transition structure	ΔH_{rel}	$\Delta\Delta H_{rel}$	n_i	ν_i	ZPE	$\Delta H^{\ddagger}$[b]
TS[(*R,M*)-**12** → (*R,P*)-**12**]$_A$	−21.1	≡0	1	60.9	427.2	16.8
TS[(*R,M*)-**12** → (*R,P*)-**12**]$_B$	−16.6	4.5	1	107.9	426.8	21.3
TS[(*S,P*)-**12** → (*S,M*)-**12**]$_A$	−19.2	1.9	1	66.4	427.0	18.4
TS[(*S,P*)-**12** → (*S,M*)-**12**]$_B$	−19.0	2.1	1	63.4	426.8	18.6
TS[(*R,M*)-**13** → (*R,P*)-**13**]$_A$	−7.1	≡0	1	56.2	427.3	18.3
TS[(*R,M*)-**13** → (*R,P*)-**13**]$_B$	−6.0	1.1	1	76.6	426.9	19.4
TS[(*S,M*)-**13** → (*S,P*)-**13**]$_A$	−2.8	4.3	1	57.7	427.4	20.5
TS[(*S,M*)-**13** → (*S,P*)-**13**]$_B$	−2.4	4.7	1	71.4	427.0	20.9

[a] ΔH_{rel} values relative to (*M*)-**10**. [b] $\Delta H^{\ddagger}$ values are related to the corresponding minima.

The Second Hydride Transfer. From this configurative instability of the intermediates **12**, **13**, and **14**, it is clear that—different from related reactions with chiral *N*-nucleophiles[5]—the first hydride-transfer reaction cannot be the chirality-determining step of the overall reductive ring-opening process. Since this process, as experimentally shown,[7,8] leads to very high asymmetric inductions, it consequently is the *second* hydride transfer reaction that may be expected to be the stereochemically

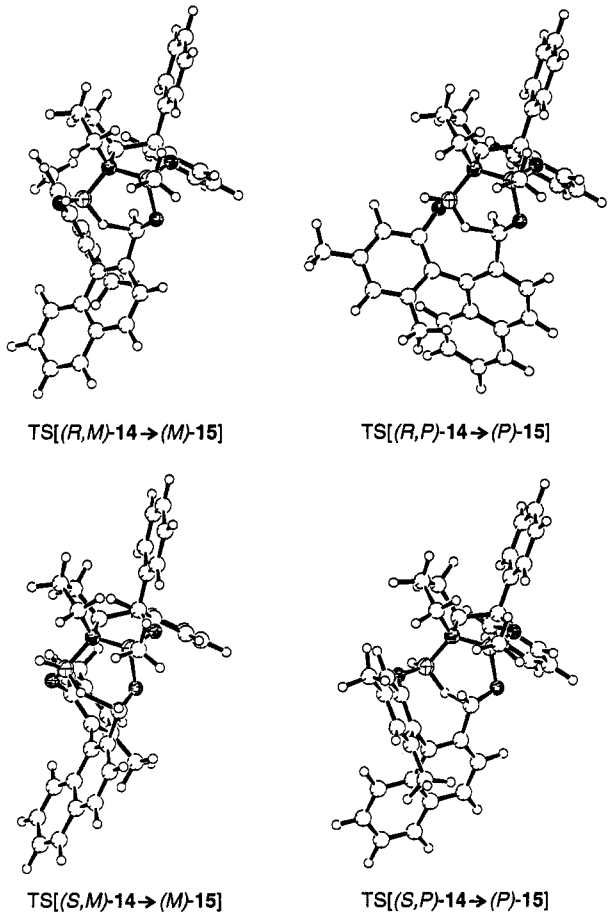

Figure 3. Transition structures for the second hydride-transfer step TS[**14** → **15**] as calculated with AM1. For reasons of clarity, the structures were plotted in a different orientation compared with the formula schemes.

deciding step, by the intramolecular reduction of possibly only one of the two atropisomeric coordinated aldehydes (*P*)-**14** or (*M*)-**14**. An investigation of the four possible hydride transfer reactions (see Figure 3 and Table 4) shows that the intramolecular attack to the boron-activated carbonyl group is distinctly favored for the *M*-helimeric form: although the *Si* attack of this *M* configurated isomer of **14** is only 0.3 kcal/mol more favored than the corresponding *Re* attack and thus energetically comparable, it is by 3.5 kcal/mol (see Table 4) lower in energy than the analogous (*P*,*Si*) attack. Still dramatically higher in energy is the transition structure for the corresponding *Re* attack to (*P*)-**14**, which is 8.5 kcal/mol more endothermic than TS[(*M*)-**14** → (*S*,*M*)-**15**]. It is interesting to note that apparently the stereoselectivity of the intramolecular attack to the aldehyde function is preferentially controlled by the configuration at the axis, whereas the topicity of the aldehyde plays an important role only for the less favored attack to the *P* atropisomer of **14** (Scheme 7).

As already mentioned above, this intramolecular reduction step requires a higher activation energy compared with the competing processes that **14** can undergo, namely the cyclization back to the lactolates **12** and their atropisomerization. The difference in energy between the preferred attack of the second hydride equivalent to (*M*)-**14** and the lowest atropisomerization pathway of (*M*)-**14** [via (*R*,*M*)-**13**, (*R*,*M*)-**12**, (*R*,*P*)-**12**, and (*R*,*P*)-**13**], to give (*P*)-**14** is 8.4 kcal/mol (respectively, 11.9 kcal for the isomerization (*P*)-**14** → (*M*)-**14**) (Tables 4 and 5).

Scheme 7

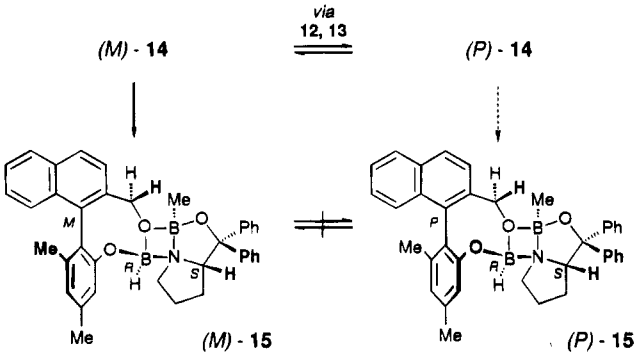

Consequently, the transiently formed aldehydes **14** must be regarded as stereochemically unstable intermediates. Hence, regardless of initially attained stereoselectivities, they will inevitably originate in the thermodynamically dictated atropisomeric ratio, with no possibility of escaping this "stereochemical leakage".

As a result of the calculations presented in this paper, it is clearly the *second* hydride transfer step that converts this atropisomeric equilibrium mixture into the stereochemically nearly homogeneous diol derivative (*M*)-**15** by an atropisomer-differentiating reduction of the configuratively unstable aldehyde adduct **14**. In this process, due to the low isomerization barriers, the remaining less reactive atropisomer (*P*)-**14** will continuously deliver the reactive species (*M*)-**14**, thus allowing to transform practically the whole material to (*M*)-**15**.

The Structure and Stereochemical Stability of the Resulting End Products 15. The stereoselective reduction of **14** leads to the diolate derivative (*M*)-**15**, the final end product of the reaction sequence before hydrolytic workup. The rigidity of the chiral polyheterocyclic ring system as part of the bridge between the aromatic systems exerts a significant influence on the relative stabilities of the atropisomers (*M*)- and (*P*)-**15**. We found the *M* isomer to be about 3.9 kcal/mol more stable than the *P* isomer in its energetically lowest conformation (see Table 3). Still, this apparently is not the reason for the high observed stereoselectivity of the reaction, since the second hydride-transfer reaction leading to (*M*)-**15** is irreversible.

The Calculated Atropisomer-Selectivity of the Overall Process. Consequently, the overall asymmetric induction of this efficient stereoselective synthesis of axially chiral compounds is the result of a kinetic resolution of the stereochemically unstable aldehydes **14**. By using the simple Eyring theory,[29] the calculation of the enantioselectivity of the reaction, based upon the activation barriers determined above, leads to an enantiomeric ratio of 99.8 to 0.2 in favor of (*M*)-**15** at 298 K.[30]

Compared with the atropisomeric ratio of *M*/*P* = 98.5/1.5 as achieved experimentally[7,8] for the ultimately isolated free diols **8**, the calculated value not only reproduces the ring-opening direction, but even offers a very good quantitative agreement, despite the complexity of the overall process and the neglect of *e.g.* solvent effects

(29) Eyring, H. *J. Chem. Phys.* **1935**, *3*, 107.

(30) For the calculation of the selectivity we neglected the activation entropy $\Delta S^{\ddagger}$ and used the following equation:

$$\frac{[(M)\text{-}\mathbf{15}]}{[(P)\text{-}\mathbf{15}]} = \frac{\exp(-\Delta H^{\ddagger}_{M,Si}/RT) + \exp(-\Delta H^{\ddagger}_{M,Re}/RT)}{\exp(-\Delta H^{\ddagger}_{P,Si}/RT) + \exp(-\Delta H^{\ddagger}_{P,Re}/RT)} = \frac{99.8}{0.2} \quad (1)$$

in our investigations. Work to include these aspects, is in progress.

Summary and Conclusions

The complete mechanistic course of the atropselective ring-opening reaction of the axially prostereogenic biaryl lactone **6** by a chiral oxazaborolidine–BH_3 reagent **9** was investigated by semiempirical AM1 calculations. Besides all previously postulated transition structures and intermediates, some unexpected stationary points were located. Especially, the different forms of the intermediate lactolates **12** and **13** were found to be important for an understanding of the complex reaction mechanism.

The major conclusion is that the stereochemically crucial step of this reaction is the *second* hydride attack on the stereochemically unstable aldehyde intermediates **14**. Hence, the overall asymmetric induction of the process does *not* depend on the selectivity of the first reduction step, as previously assumed (and still valid for *N*-nucleophiles),[5] since, by rapid intramolecular cyclization of the aldehydes **14** back to the lactolates **13/12** and rapid helimerization of these bridged biaryls, all initially obtained stereochemical information at the axis should get lost. On the other hand, this stereochemical leakage is the fundamental basis of the actually selectivity-determining step—the highly atropodiastereomer-differentiating reduction of this configuratively unstable aldehyde **14** only out of its *M*-helimeric form. The resulting calculated ratio of 99.8:0.2 in favor of (*M*)-**15** not only computationally reproduces the ring-opening direction, but even very closely matches the actual experimental value of 98.5:1.5 despite still necessary simplifications concerning activation entropies, solvent effects, etc.

An interesting practical consequence of these calculations results from the unexpectedly high importance of the "stereochemical leakage". If indeed, as predicted from the calculations, the stereochemically deciding step is the final reductive transformation of the aldehyde derivative **14** to the alcoholate **15**, it should be possible to perform the reaction not only starting from the lactones **6**, but even from racemic boron-free aldehydes related to **14**. According to this concept, the stereochemically unstable[31] aldehydes might be interesting substrates for an enantiomer-differentiating reduction to configuratively stable biaryl diols, resulting in a kinetic racemate resolution with transformation of the whole material into essentially one atropo-enantiomeric product, *e.g.* only (*M*)-**8**—a new concept for the enantioselective synthesis of axially chiral biaryl compounds. The realization of this computationally predicted novel concept is under investigation.

Acknowledgment. We gratefully acknowledge financial support from the Deutsche Forschungsgemeinschaft (Sonderforschungsbereich no. 347 "Selektive Reaktionen Metall-aktivierter Moleküle", project B-1) and from the Fonds der Chemischen Industrie. We also thank U. Dauer and K.-P. Gulden for fruitful discussion and valuable technical support and S. Güssregen for proofreading the manuscript.

JO9511206

(31) Bringmann, G.; Hartung, T. *Liebigs Ann. Chem.* **1994**, 313.